Graduate School of Pure and Applied Sciences

Development on Optical Pump-probe Scanning Tunneling Microscopy for Probing Spin Dynamics
(光学的ポンププローブ走査トンネル顕微鏡法の開発とスピン計測への応用)

Wang Zihan

Doctoral Program in Applied Physics
Student ID: 201630112
Doctor of Philosophy in
Engineering
Advised by Prof. Hidemi Shigekawa
Signature

Summary

1. Background

Scanning Tunneling Microscopy (STM), as one of the major breakthroughs in physics in late 20th century, both scientifically and technically, has opened a whole new prospect in surface and nano-science. Generally speaking, empowered by this microscope, for the first time ever, researchers were able to visualize atoms in real space thanks to the ultimate spatial resolution (sub-nm) of STM, thus, atomic scale characterization on various types of physical and chemical properties at nanoscale can be achieved using STM.

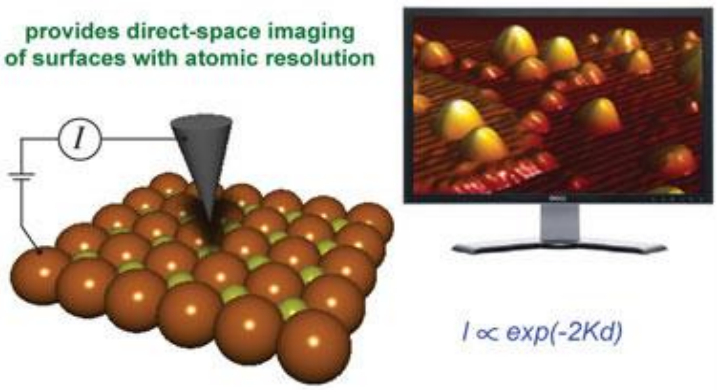

Figure 1 | Schematic illustration on STM. Atomic resolution can be obtained by measuring the tunneling current flowing between a conductive sharp tip and (semi-) conductive sample beneath it. Figure is adopted from *the website of SCISS, University of St. Andrews, United Kingdom.*

Simply speaking, as shown in ***Figure 1***, the basic concept of STM is to take advantage of the relationship between the quantum tunneling effect with distance, by putting an ultra-sharp conductive tip above a (semi-) conductive sample, when tip and sample are brought sufficiently close, by applying a bias voltage across the nanoscale tip-sample junction, current will be flowing in between even though they are not physically connected. This is, without a question, a beautiful representation of the well-known quantum tunneling effect that used to appear only on textbooks. The current flowing between tip and sample is called tunneling current, which is, highly confined in real space and extremely sensitive to tip-sample distance, giving us local information of the sample with sub-nm spatial resolution.

Ever since STM was invented in 1982, as a groundbreaking nanoscale measurement technique, great research interests had been drawn, either using STM to discover nanoscale physical and chemical phenomena that could not be directly observed in previous ages, or implementing fancy new ideas on STM to improve its performance and varieties. Among these STM-based techniques, one of the most exciting one is to use STM to study spin properties.

We all know that, spin, as an intrinsic property of particles including electrons and nucleus, is one of the greatest discoveries in modern quantum mechanics. Scientists and engineers have been trying to understand spin properties from different perspectives and make use of those properties in order to revolutionize modern electronics. As we know, modern electronics and computers are gradually approaching their technical limits, as it was predicted by the famous “Moore’s

Law", further downscaling on the size of electronic circuits will be barricaded due to the heat effect and leakage current, especially when it goes into the quantum regime. Alternatively, spin is considered as novel candidates for new generation of faster, smaller and more efficient computational devices, that is, a generation of "Spintronics" and spin-based quantum computation.

However, to make full use of spin for future applications, first, understanding spin both theoretically and experimentally is the priority, especially at nanoscale. Thus, great efforts had been made to characterize local spin properties using STM-related techniques, such as "Spin-polarized STM" (SP-STM), in which ultra-sharp conductive tip is coated with a thin layer of magnetic materials, makes it sensitive to single atomic level spin properties in addition to surface topography; and "Electron Spin Resonance STM" (ESR-STM), in which radio frequency (RF) wave is coupled with STM, to detect dynamical behaviors such as spin Larmor precession on frequency and spatial domain. These STM-based techniques, had been demonstrated to be very useful to study spin properties at atomic scale. Several inspiring experiments using these techniques to measure or even manipulate spin did show solid evidences that STM can be used for studying nanoscale spin properties.

2. Purpose of this research

As it was previously introduced, the ultimate atomic level spatial resolution makes STM a suitable tool to study nanoscale physical and chemical properties, including spin-related phenomena. nevertheless, it is the fact that the temporal resolution of STM is very much limited. Basically, STM tunneling current is very small, so generally amplification is required, and the temporal resolution of STM is determined by the bandwidth of amplification electronics, namely, the current pre-amplifier. Thus, there must be tradeoff between bandwidth and amplification gain. Thus, for STM, the temporal resolution is essentially pre-amplifier-bandwidth-limited and it is on the order of ~1ms. Even though excellent spatial resolution can be offered by STM, the ms level temporal resolution makes it a rather slow-speed measurement technique, so that tremendous amount of intriguing nanoscale quantum dynamical behaviors such as transient electron or nuclear spin dynamics which time-scales are below ms level, cannot be resolved by STM.

In the past few decades, researchers have been making great efforts in improving temporal resolution of STM, and one of the most successful solutions was originally proposed and demonstrated by our group, that is, a combination between ultrafast optical pump-probe (OPP) technique and STM, namely, OPP-STM. Previously, OPP-STM has been proved to be powerful in probing sub-ps to ms carrier recombination dynamics in semiconductors at nanoscale, including carrier trapping dynamics into a gap state made of single dopant atom, and carrier drift & diffusion dynamics in semiconductors, with both high temporal and spatial resolution simultaneously.

Based on this OPP-STM concept, the purpose of this research is focused on developing an OPP-STM platform which can be used to probe electron and nuclear spin dynamics, with sufficiently high temporal and spatial resolution at the same time.

3. Development and application on time-resolved STM for probing spin dynamics

(a). Development and application on OPP-STM for probing electron spin dynamics

To establish a novel time-resolved STM system that can be used to probe electron spin dynamics both in time- and spatial-domain, the most important issue to be solved has to be electron spin excitation and detection under OPP-STM scheme.

As we know, in semiconductors, circularly polarized light can effectively excite electron spins due to the optical selection rule, which is, angular momentum transferring from circularly polarized photons to electrons. Also, it is important to emphasis that for non-spin-polarized STM, tunneling current is solely sensitive to local carrier density, by knowing these basics, in the following part, how electron spin dynamics can be probed using OPP-STM will be unfold step by step.

Generally, in OPP-STM for probing electron spin dynamics, both pump and probe pulses are tuned to be circularly polarized, and the polarization state is being modulated between "right-handed circularly polarization" (R-light) and "left-handed circularly polarization" (L-light), respectively, this is realized by *λ/4* waveplates and ultrafast Pockels cells controlled by one home-build, Complex Programmable Logic Device (CPLD)-based logic circuit with exquisitely designed algorithms. It is indeed a very unique approach that there is a slight modulation frequency difference being intentionally introduced between pump and probe pulses, as shown in ***Figure 2a***. For example, for pump pulses, the modulation frequency is 1MHz; while for probe pulses, the modulation frequency is slightly detuned with respected to pump modulation, for e.g. 0.999MHz, consequently, here the frequency difference Δf = 1MHz - 0.999MHz = 1kHz will give rise to a consecutive phase shifting between pump and probe pulses. As it is indicated in ***Figure 2b***, there will be two distinct "polarization modes" involved due to the phase shifting. One is called "co-circularly polarization" mode, in which the polarization state of pump and probe pulses are always the same; another one is called "counter-circularly polarization" mode, in which the polarization state of pump and probe pulses are always in opposite. As a result, suppose that the system is started with "co-circularly polarization mode", then within 1ms (1/1kHz), then system undergoes a well-defined polarization mode transition from the "co-circularly polarization mode" to "counter-circularly polarization mode" and again back to "co-circularly polarization mode", as shown in ***Figure 2c***.

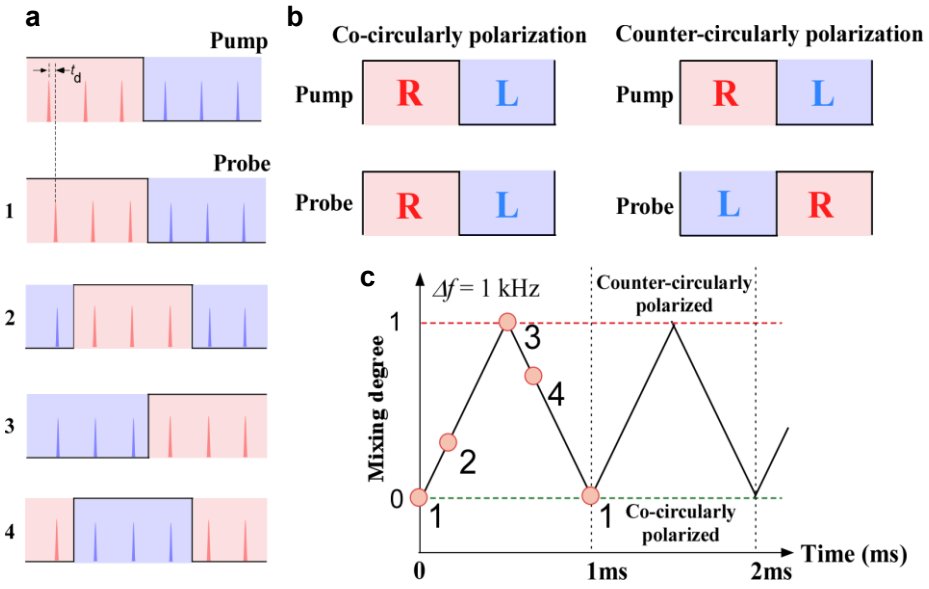

Figure 2 | Schematic illustration phase relationship between pump and probe pulses, in terms of polarization states. (a). By giving modulation frequency difference Δf (1kHz here) between pump and probe pulses, a consecutive phase shifting will be occurred. Red pulses: right-handed circularly polarized pulses; blue pulses: left-handed circularly polarized pulses, t_d: delay time between pump and probe pulses. **(b).** Due to the phase shifting as it was indicated in **(a)**, there are two distinct "polarization modes" involved, namely, "co-circularly polarization (co-CP)" mode and "counter-circularly polarization (counter-CP)" mode, respectively, Here R: right-handed circularly polarized pulses; L: left-handed circularly polarized pulses, respectively. **(c).** polarization mode is being modulated at 1kHz. Points with numbers are corresponding

Next let's take a look at why this polarization modulation technique is necessary and essential in functionalizing OPP-STM for electron spin dynamics measurement, regarding to spin excitation and detection.

The working mechanism on OPP-STM is explicitly shown in ***Figure 3***. Suppose that both pump and probe laser pulses are tuned to be above bandgap in excitation energy, with respect to the target semiconductor sample. And STM tip-sample junction is illuminated by colinearly aligned pump and probe pulses (with variable delay-time t_d in between). As shown in ***Figure 3a***, in "co-circularly polarization mode" after spin excitation by pump pulse (here, supposedly, pump pulse is R-light = electrons with down-spins are excited): at very short delay time, for e.g. delay time t_d < spin lifetime τ_s, absorption of probe pulse (L-light) will be suppressed, as there are no more rooms for down-spin electrons to be excited, that is to say, the sample has been optically "bleached" in terms of certain spin-polarized electrons; at very long delay time, for e.g. delay time t_d > spin lifetime τ_s, the absorption of probe pulse (L-light) will not be impeded as pump-excited spin-polarized electrons have been relaxed. Thus, photo-carrier density n_{ex} is exponentially increasing as a function of

delay time t_d. In ***Figure 3b***, for "counter-circularly polarization mode", after spin excitation by pump pulse (here, supposedly, pump pulse is R-light = electrons with down-spins are excited): at very short delay time, for e.g. delay time t_d < spin lifetime τ_s, the absorption of probe pulse (L-light) will not be impeded because it excites spin-polarized electrons with opposite orientation with respect to pump pulse; at very long delay time, for e.g. delay time t_d > spin lifetime τ_s, the absorption of probe pulse (L-light) will be suppressed because pump-excited spin-polarized electrons have been relaxed, which indicates, some of the relaxed electrons, are in up-spin states, preventing the absorption of probe pulse. Thus, photo-carrier density n_{ex} is exponentially decreasing as a function of delay time t_d. As it can be seen, these two polarization modes contribute differently to the photocarrier density n_{ex}, as a function of delay time, and the differential photocarrier density Δn_{ex} can be reflected in STM tunneling current via polarization modulation. As represented in ***Figure 3c***, if we define the co- (counter-) CP-determined tunneling current to be $I^{co}(t_d)$ ($I^{counter}(t_d)$), as STM tunneling current I is proportional to n_{ex}, the relaxation of electron spin can be reflected in the lock-in detected differential tunneling current, which can be qualitatively represented as: $\Delta I(t_d) = I^{counter}(t_d) - I^{co}(t_d)$.

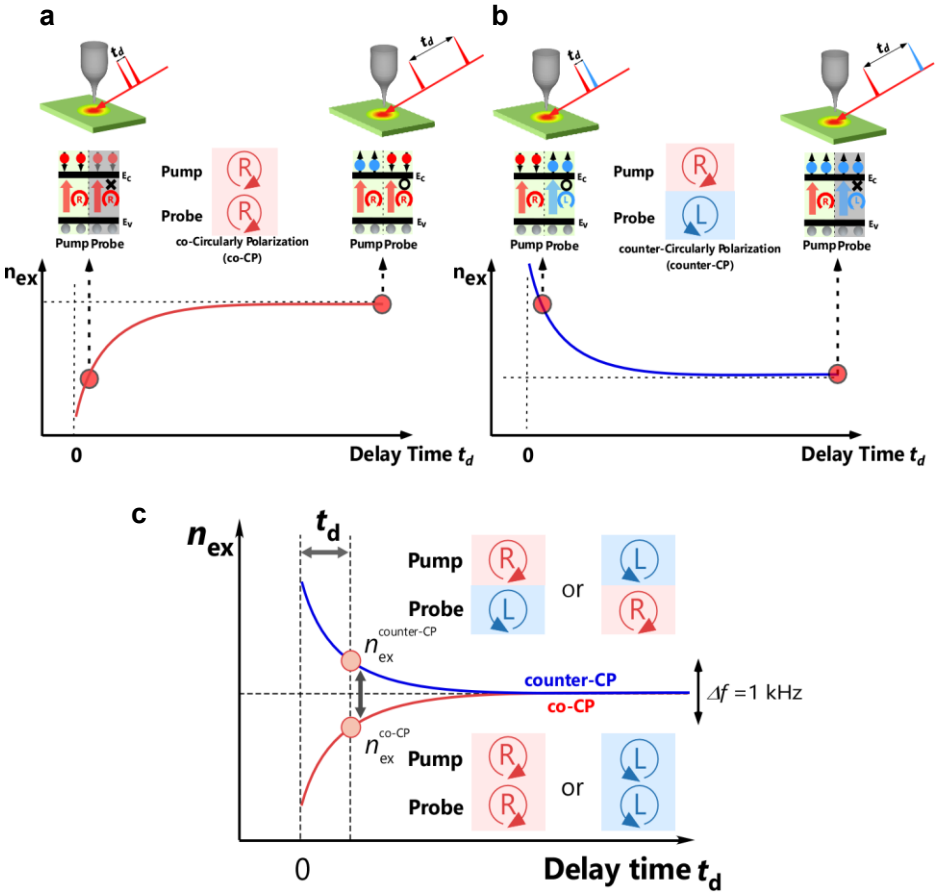

Figure 3 | Working mechanism of polarization modulation in OPP-STM for electron spin dynamics measurement. (a). In "co-circularly polarization mode", with a super-bandgap illumination, after pump pulse excitation, the absorption of probe pulse will be suppressed ($t_d < \tau_s$) or unimpeded ($t_d > \tau_s$). Here for simplicity, pump pulse is set to be R-light. **(b).** In "counter-circularly polarization mode", with a super-bandgap illumination, after pump pulse excitation, the absorption of probe pulse will not be suppressed ($t_d < \tau_s$) or impeded ($t_d > \tau_s$). Here for simplicity, pump pulse is set to be R-light. **(c)**. $\Delta n_{ex}(t) = n_{ex}^{counter}(t) - n_{ex}^{co}(t)$ can be reflected in the lock-in-detected STM tunneling current, offering information on spin dynamics as a function of delay time t_d.

There are several additional advantages using this special polarization modulation technique, first, since no optical chopper is used (which is commonly applied in ultrafast OPP measurements for modulation), there is no active modulation on laser intensity, there is no active modulation on laser intensity which indicates that tip-sample distance will be relatively stable even if intense laser pulse in irradiating on the junction. What's more, as polarization can be unintentionally modulated due to the polarization dependence of reflectance on optics, this passive laser intensity modulation can also be minimized as much as possible since the number of R-light equals to that of L-light in this high-speed polarization modulation technique. Last but not least, in actual OPP-STM system, pump and probe pulses are coming from two femtosecond laser sources, and they are synchronized in terms of repetition rate (80MHz here) in a typical "master-slave" configuration. This can also offer us a great technical advantage that the after-synchronizing phase relationship between

two femtosecond lasers can be easily tuned, resulting in providing a relatively long delay time (up to 6.25ns = ½ pulse interval) with excellent delay resolution (~130fs), thus, NO mechanical delay stage is deployed in this OPP-STM scheme. However, due to the electronic jitter of synchronization circuit, overall temporal resolution will be compromised to a certain extent, which is estimated to be 1ps after synchronization.

Now let's take a look at experimental results obtained by this OPP-STM, on electron spin dynamics measurements. We have successfully measured spin Larmor precession under external magnetic fields as shown in ***Figure 4a***. Larmor precession frequency can be defined as: $f = g\mu_0 B/\square$. Here g is the electron g-factor; μ_0 is the Bohr magneton; B is the applied external magnetic field; $\square$ is the Dirac constant. The g-factor for an electronic state in a semiconductor is highly sensitive to the characteristics of local electronic structures as well as to the associated band, that is why it is an important parameter in understanding quantum dynamics in materials and devices. By using OPP-STM, with increasing external magnetic field, it was clearly identified that the oscillation frequency of spin precession is also increased, meanwhile, g-factor and spin lifetime can be extracted from these OPP-STM spectra. This is, the first time ever on successful probing of precession dynamics of optical orientated spins. In ***Figure 4b***, experimental results on calibrating in-plane spatial resolution of OPP-STM are presented. Here a GaAs/AlGaAs multiple quantum well nanostructure was used, by doing a cross-section scan over an area where 3nm and 6nm quantum wells are located, one can clearly see that the laser excited electron spin signal only appears on quantum wells, this is a solid evidence which supports that the in-plane spatial resolution of OPP-STM is ~1nm in real space.

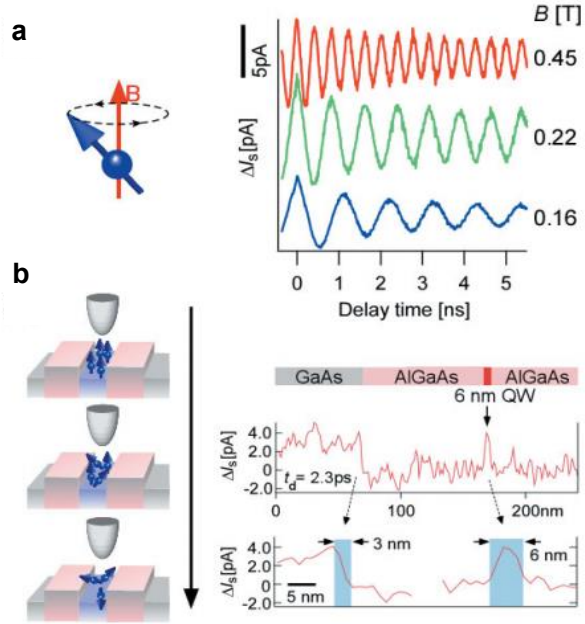

Figure 4 | electron spin dynamics probed by OPP-STM on GaAs and its nanostructures. (a). Electron spin larmor precession monitored by OPP-STM on moderately doped n-type GaAs sample (doping concentration ~ 2×10^{16} cm^{-3}) at low temperature (2.5K) with in-plane external magnetic field. **(b).** Electron spin signal obtained on GaAs/AlGaAs multiple quantum well nanostructure at 300K, revealing that the in-plane spatial resolution of OPP-STM is ~1nm.

Next, I focused on measuring electron spin dynamics in Mn-doped GaAs system. Diluted Magnetic Semiconductors (DMSs), such as Mn-doped GaAs, in which some atomic sites are substituted by transition metal atoms, had been drawing great research attentions in past few decades. Unlike conventional nonmagnetic semiconductors, DMSs have both ferromagnetic and semiconductor properties below the Curie temperature T_c, which is expected to be increased even up to room temperature, and are widely acknowledged as an ideal platform for exploring potential for practical applications in spintronics. For Mn-doped GaAs, especially at nanoscale, the surface Mn alignment are closely related to the origin of ferromagnetism and critical in determining T_c. Here by using OPP-STM to measure electron spin dynamics on a cleaved GaAs (110) surface deposited with Mn adatoms, time-resolved, surface-mediated spin dynamics are obtained for the first time ever, showing some thought-provoking properties as well as demonstrating that the OPP-STM system is surface sensitive.

All experiments were carried out at 300K, Mn adatoms were deposited on an in-situ cleaved GaAs (110) surface using evaporation method. ***Figure 5*** shows the STM topographies on Mn-deposited GaAs surface with different deposition time. Mn denstiy on surface was increased linearly with respect to depostion time, and it can be estimated by counting the numbers of Mn adatoms. Next, OPP-STM measurments on Mn-deposited GaAs were taken. The experiment shows very thought-provking results when surface Mn density is increaed, as shown in ***Figure 6a*** and ***6b***, it can be clearly seen

that, a non-monotonic behavior on electron spin lifetime as a function of surface Mn density has been identified: at first, when Mn density was incresed, the measured spin lifetime was also increased; however, after reaching a peak value (deposition time ~60s), spin lifetime started to decreased, until the measurement stopped at the relative large surface Mn density, where surface was almost coverred by Mn atatoms. This very intruging result can be expalined as follows: especially in n-type GaAs, such as the sample used in this experiment, at room temperature (300K), the dominating spin relaxation mechanism is represented by Dyakonov-Perel (DP) mechanism. Owning to spin-orbit interaction, microscopic magnetic field is acting upon electron spins, in which the impurity atoms included in the sample playing a deterministic role in electron spin relaxation process. Namely, electron spins are scattered off by impurities, and spin relaxation occurs during two subsequent scattering events, therefore, in DP mechanism, spin lifetime (τ_s) is inversely proportional to the momentum lifetime (τ_p), that is, $\tau_s \sim \tau_p^{-1}$. Whereas in p-type GaAs, particularly when hole concentration is relatively high, at room temperature, the dominating mechanism leading to electron spin relaxation is called Bir-Aronov-Pikus (BAP) mechanism, in which electrons lose their spin polarization via ultrafast exchange interaction with holes, in this case, electron spin lifetime is inversely proportional to hole density (n_h), $\tau_s \sim n_h^{-1}$.

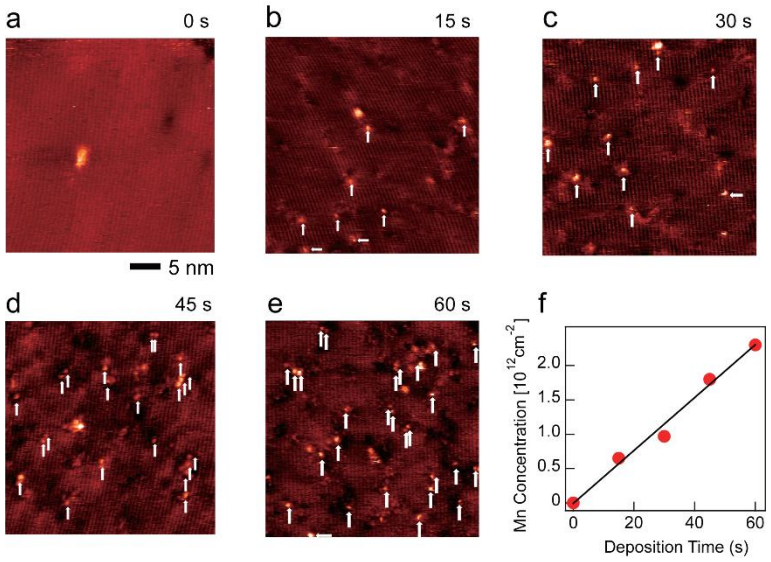

Figure 5 | STM images on GaAs (110) surface with different Mn densities. (a) to **(e).** STM topographies of in-situ cleaved GaAs (110) surfaces (n-type GaAs with doping concentration ~ 1×10^{18} cm^{-3}, in which good conductance (higher STM topography quality) can be offered) for different Mn deposition times. **(f).** Estimated surface Mn density (unit = $10^{12}cm^{-2}$) as a function of deposition time. Red dots are Mn densities evaluated from STM topographies **(a)** to **(e)**), black solid line is for guidance.

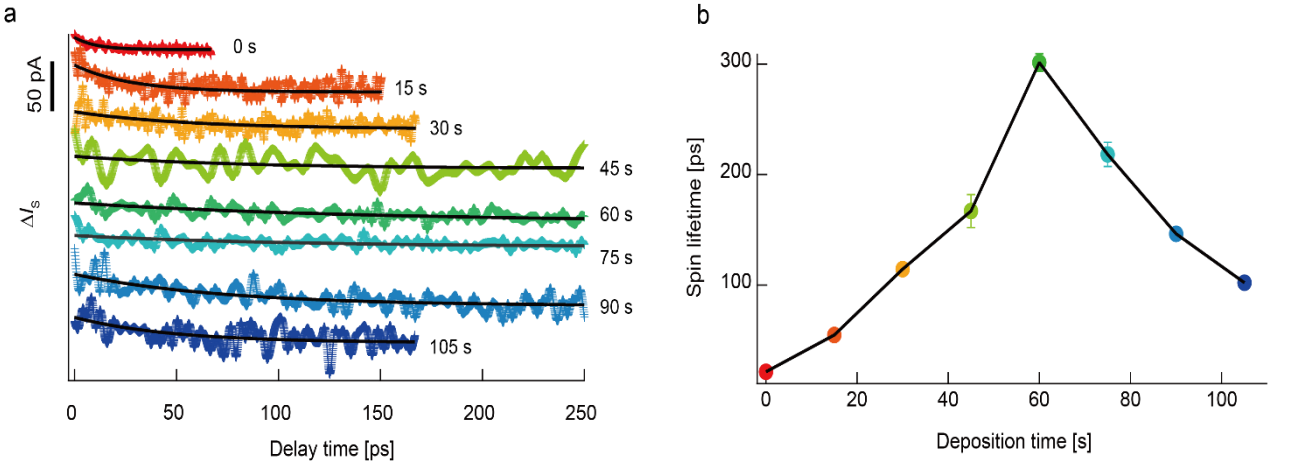

Figure 6 | Electron spin lifetime at different surface Mn densities obtained by OPP-STM. (a). Mn-density-dependent OPP-STM spectra, obtained for the n-type GaAs with doping concentration ~ (3.8~6.2) $\times10^{16}$ cm^{-3}, in which the offset manually adjusted for each spectrum. Black lines are fitting curves with a single exponential function, and the lifetimes obtained were, from top to bottom, *21 ± 2 ps, 55 ± 3 ps, 114 ± 5 ps, 167 ± 15 ps, 301 ± 8 ps, 219 ± 11 ps, 164 ± 4 ps, 102 ± 5 ps*, respectively. **(b)**. Spin lifetimes, which were obtained from the fitting curves in **(a)**, plotted as a function of Mn deposition time. The peak lifetime was reached at a deposition time of 60 s, corresponding to a Mn density of ~ 2.3×10^{12} cm^{-2}. Same colors are used in **(a)** and **(b)**.

From this perspective described above, because Mn adatoms on GaAs (110) surface at 300 K act as paramagnetic impurities in the system we investigated, the rate of scattering between electrons and Mn atoms, which suppresses the spin relaxation, increases with increasing Mn density, and the spin lifetime is initially extended due to DP mechanism. However, with a further increasing of surface Mn density, as most of the Mn adatoms replace Ga sites and act as acceptors, the effective (p-) doping on the surface induces a transition in the target sample, namely, from a lightly doped n-type semiconductor to a hole-rich p-type one at and near the surface. Therefore, the decrease in the spin lifetime after it reached the peak position can be attributed to the effect of BAP mechanism. That is, with a relatively high surface Mn density, as the BAP mechanism is significantly enhanced, the increased competition between the DP and BAP mechanisms leads to an overall decrease in the spin lifetime. This effect of DP-BAP competition upon increasing the effective p-type doping concentration has been theoretically predicted to occur in a similar p-type GaMnAs quantum well system. This is the first direct observation of the transition of the spin relaxation process from the DP mechanism to the BAP mechanism.

To evaluate the *z*-directional (perpendicular to the sample surface) spatial resolution of OPP-STM, conventional OPPR (Optical Pump-probe Reflectivity) measurements were carried out on identical Mn-deposited surfaces using the same

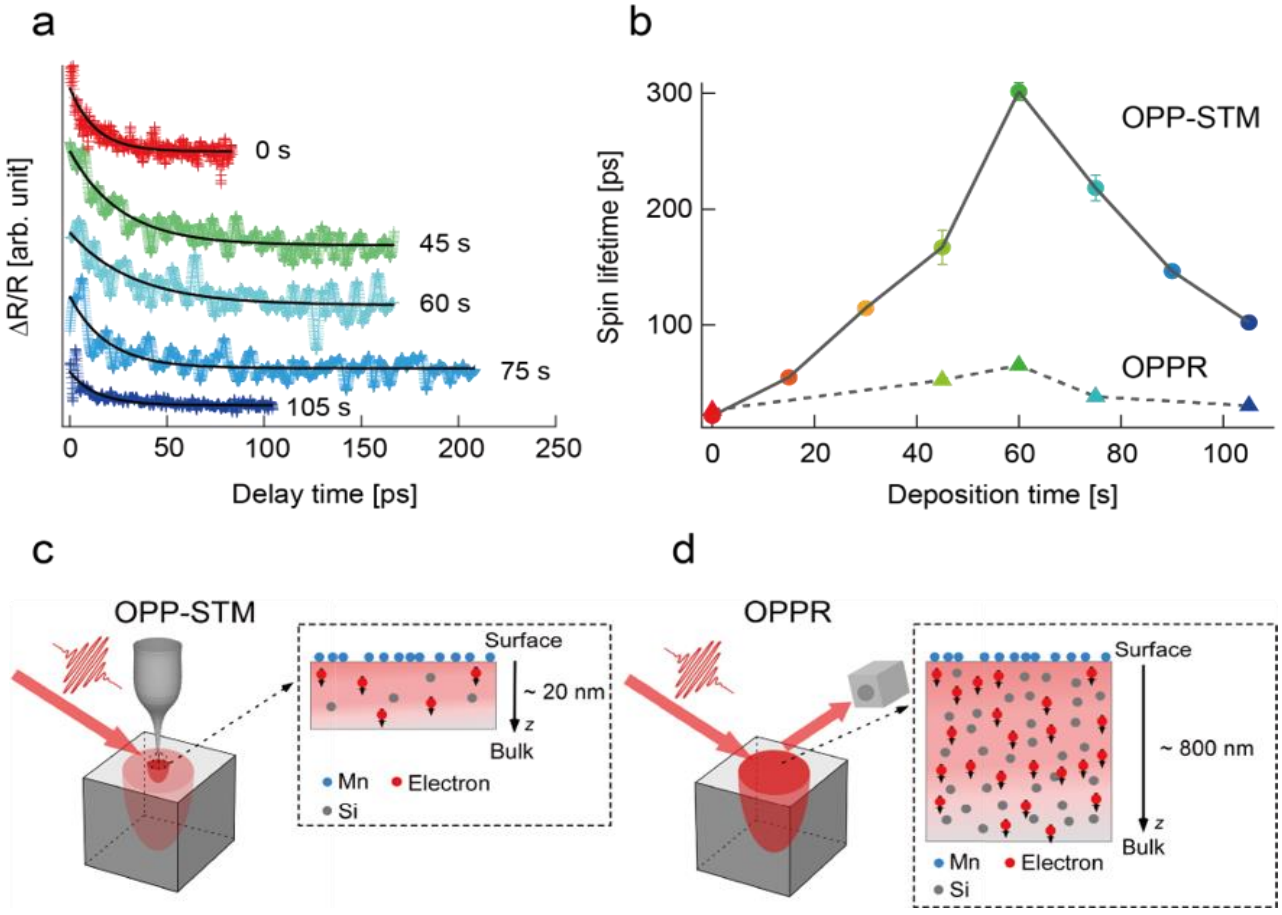

Figure 7 | Comparison between spin lifetimes obtained by OPP-STM and OPPR methods. (a). Mn density dependent OPPR spectra. From top to bottom, the deposition time (Mn density) was increased, with the offset manually adjusted for each spectrum. Black lines are fitting curves and the lifetimes obtained were, from top to bottom, 26 ± 1 ps, 52 ± 1 ps, 65 ± 2 ps, 38 ± 1 ps, 30 ± 1 ps, respectively. **(b)**. Comparison of the deposition-rate dependence of the spin lifetime obtained by the two methods. The results obtained by OPP-STM shown in Figure. 8b are shown together for comparison. **(c).** Schematic illustration of the probing area in OPP-STM measurement. **(d)**. Schematic illustration of the probing area in OPPR measurement. The measured spin lifetime was almost entirely determined by the bulk, and the Mn-deposited surface had very little effect. Here, blue balls, Mn atoms; red balls, electrons; gray balls, Si dopant atoms. For simplicity, only electrons with down spins are shown here.

setup as for OPP-STM with the STM tip extracted from the sample and using photodetector located outside STM UHV chamber to collect light reflected off sample surface. As it can be seen from ***Figure 7a*** and ***7b***, the tendency of the nonlinear lifetime observed by OPP-STM was much less pronounced in the case of OPPR measurement. This is considered to be due to the difference in probing depth between OPP-STM and OPPR measurements.

As explained in ***Figure 7c*** and ***7d***, In OPP-STM of a semiconductor, its signal mainly originates from the area where tip-induced band bending (TIBB) occurs, namely, OPP-STM is highly sensitive to the surface dynamics. The TIBB depth depends on parameters such as tip radius, tip-sample distance, bias voltage, and doping concentration. Considering the experimental conditions, the effective TIBB z-depth was estimated to be ~20nm, Whereas in OPPR measurement, the in-plane spatial resolution was determined by the laser spot size of 50μm, the spatial resolution perpendicular to the surface (z-direction) depends on the optical penetration depth, which was ~800nm in current case and much larger than that of OPP-STM. In the Mn-deposited GaAs (110) system, Mn atoms existed only on the surface, acting as impurities and also acceptors, and Mn ion diffusion to the bulk was suppressed during the OPP-STM measurement because the sample was reversely biased (positive sample bias). Therefore, with increasing surface Mn density, the nonlinear spin lifetime behavior, which was determined by both the DP and BAP mechanisms, is considered to only occur in the area near the surface. In contrast, in the OPPR measurement, the time-resolved spin dynamics signal was obtained from deep inside the bulk, thus the nonlinear contribution from the surface was greatly reduced.

In conclusion, the OPP-STM system has been demonstrated to be very powerful, and surface sensitive in characterizing electron spin dynamics under various experimental condition, with high temporal and spatial resolution simultaneously.

(b). Development and application on OPP-STM for probing nuclear spin dynamics

Based on OPP-STM for probing electron spin dynamics, I proposed a new OPP-STM aiming at probing nuclear spin dynamics at nanoscale. Compared with electron spin, nuclear spin may have greater potential in actual applications since generally its lifetime is much longer than that of electron spin. Longer spin lifetime is particularly desirable for applications such as spin manipulation. However, in OPP-STM scheme, it is indeed required to consider how nuclear spin can be excited and detected.

Nuclear spin, is actually not a totally isolated, theoretical studies and also experimental evidences pointed out that, electron spin and nuclear spin are essentially connected with each other, under some certain circumstances, the interaction between electron and nuclear spin is called "hyperfine interaction". For e.g. in semiconductors, specially at low temperature, for confined electrons (electrons trapped in quantum wells or dots, or electrons that are bound to donors), the hyperfine interaction is significant, as a result, suppose that electron spin are polarized (for e.g. by a circularly polarized light), then nuclear spin can also be, yet indirectly, polarized due the hyperfine coupling. As shown in ***Figure 8***, this is called

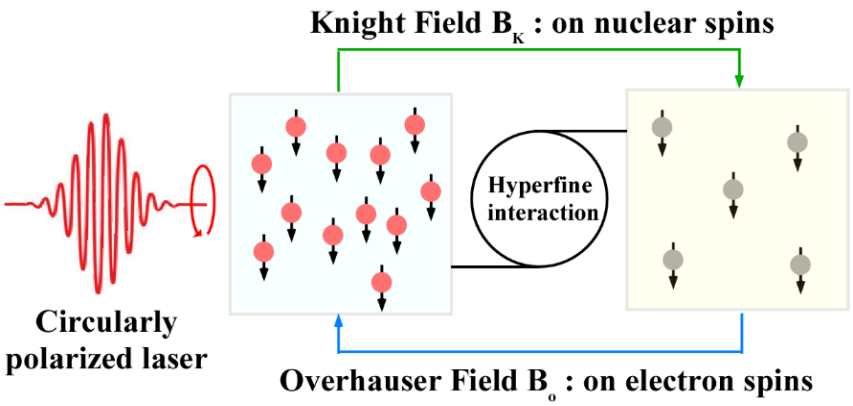

Figure 8 | Schematic illustration on hyper-polarization for exciting nuclear spins in semiconductors. Here right-handed circularly polarized laser is used as an example. At first, electron spin (down spin here) can be polarized based on optical selection rule, then owing to the hyperfine interaction between electron spins and nuclear spins, nuclear spin can be indirectly polarized. Meanwhile, two hyperfine magnetic fields are also produced, namely, Knight field B_K that affects nuclear spin; Overhauser field B_o that affects electron spin, respectively. Note that this hyper-polarization mechanism is effective only if hyperfine interaction is significant (for e.g. at low temperature on some confined systems)

"hyper-polarization" mechanism. On top that, due to the hyperfine coupling, there are hyperfine magnetic fields involved. One hyperfine magnetic field that acting upon nuclear spin is called Knight field, which is essentially generated by aligned electron spin; another hyperfine magnetic field that acting back upon electron spin is called Overhauser field, which is essentially generated by aligned nuclear spin. In general, Knight field is much smaller than Overhauser field in terms of magnitude.

Now it is clear that nuclear spin can be indirectly but effectively polarized by firstly polarizing electron spin under certain conditions, then it is possible to excite nuclear spin and then detect its dynamics in OPP-STM scheme. From this perspective, as shown in ***Figure 9***, based on the OPP-STM for probing electron spin dynamics, additional "initialization pulses" are required to build up nuclear spin by continuously polarizing electron spin at first. Literally, the "initialization pulses" are circularly polarized laser pulses with fixed polarization state, either right-handed circularly or left-handed circularly, and the length of "initialization pulses" can be tuned from 1ms up to 30 minutes offering us enough degree of freedom to choose the duration of initialization pulses. Immediately after "initialization pulses", both pump and probe pulses are going back to the "modulation pulses", namely, exactly as what was used for probing electron spin dynamics. This design was realized by developing a whole new algorithm embedded in CPLD logic circuits, allows us to probe electron spin dynamics under nuclear spin influence, for e.g. once nuclear spins are polarized, the hyperfine magnetic field (Overhauser field) will be generated and affect back upon electron spins, thus, electron spin dynamics, will be modified by this nuclear influence, by looking at the change on electron spin dynamics with and without nuclear spins polarization, or changing the polarity of nuclear polarization, we can indirectly extract information on nuclear spin dynamics.

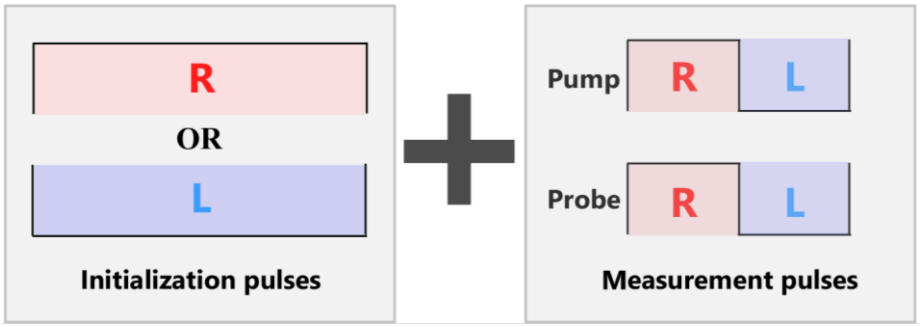

Figure 9 | Basic concept on nuclear spin excitation and spin dynamics measurement in OPP-STM. unlike OPP-STM for electron spin dynamics measurement, here, initialization pulses are necessary to polarize nuclear spin by firstly polarizing electron spin via hyper-polarization. For initialization pulses, circularly polarization state is fixed right-handed circularly polarized (R) or left-handed circularly polarized (L), also the length (time duration of initialization pulses) can be adjusted. Then, after initialization pulses, system goes back to polarization modulation mode (measurement pulses), as previously used for OPP-STM on electron spin dynamics measurement.

Next, OPPR experiments using the newly designed nuclear spin excitation method were carried out, to testify if the system works functionally as expected. A moderately doped, Metal-Insulator-Transition (MIT) GaAs (2×10^{16} cm^{-3}) sample were used at low temperature (2.5K), the donor-bound electron system in such a sample has been proved to be manifesting significant nuclear-electron spin hyperfine interaction, which is a simple and novel platform for system testing. However, though the newly designed algorithm has been confirmed to be functional, it turned out that there was a technical problem involved when system changed between "initialization pulses" and "measurement pulses", the laser spots were slowly deviated from overlapped position due to the thermal instability of ultrafast Pockels cells, thus, an artifact signal appeared. Experimental evidences on this issue as well as the solution (by re-designing optical setup and deploying active beam stabilization systems) will be addressed in detail in the dissertation.

(c). Development on nanosecond laser based OPP-STM system for probing carrier and spin dynamics.

In previous OPP-STM designs, femtosecond OPP-STM, though it has been proved to be very powerful in resolving transient dynamics, it is undeniable that the sophisticated design makes it budget-demanding and skill-requiring.

Therefore, I put forward a new idea using nanosecond pulse lasers to realize a budget-friendly, easy-to-use, maintenance-free OPP-STM system with ns temporal resolution. Two externally triggerable nanosecond pulse lasers controlled by a single home-brew, FPGA control board with newly designed algorithms, in which synchronization, delay time scanning, repetition rate tuning, and laser modulation can be realized, consequently, the optical setup has become super easy to handle with.

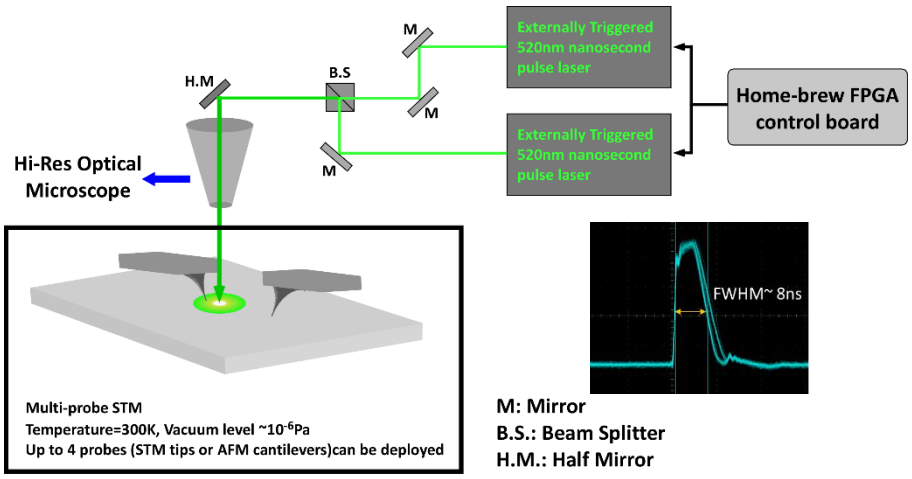

Figure 10 | illustrations on nanosecond OPP-STM combined with multi-probe STM platform. Two externally triggerable nanosecond lasers are controlled by a FPGA board, laser pulses are tightly focused on sample surface via the hi-res optical microscope. Multi-probe STM can be operated either using STM tips or AFM cantilevers (as an example, 2 AFM cantilevers are used here). Characterization on laser pulse width (inset) indicates that the temporal resolution of this system is ~ 8ns

Moreover, this time, the nanosecond OPP-STM is implemented with a multi-probe STM platform, as shown in ***Figure 10***. our newly modified multi-probed STM can offer an optical access through the hi-resolution optical microscopy on top of sample stage, giving an excellent focus quality which is particularly important for the current low power nanosecond pulse lasers (5μW at 25KHz repetition rate), also, the multi-probe STM system combined with OPP technique can be used to study surface side, in-plane transient dynamics, which is, highly preferable some newly emerged mono-to-multi-layered Transition Metal Dichalcogenide (TMD) materials or topological insulators. Here, as a demonstrative experiment, carrier recombination dynamics on bulk WSe_2 sample has been investigated, particularly when 2 AFM cantilevers were both contacted on sample surface with separation < 5μm, a very long component in carrier lifetime was observed and the bias voltage dependence showed interesting non-linear behavior as shown in ***Figure 11***. The physical origin of this long component is still unclear but we have reason to believe it might be related to the deep level defect trapped carriers, which can be further confirmed by deep level transient spectroscopy.

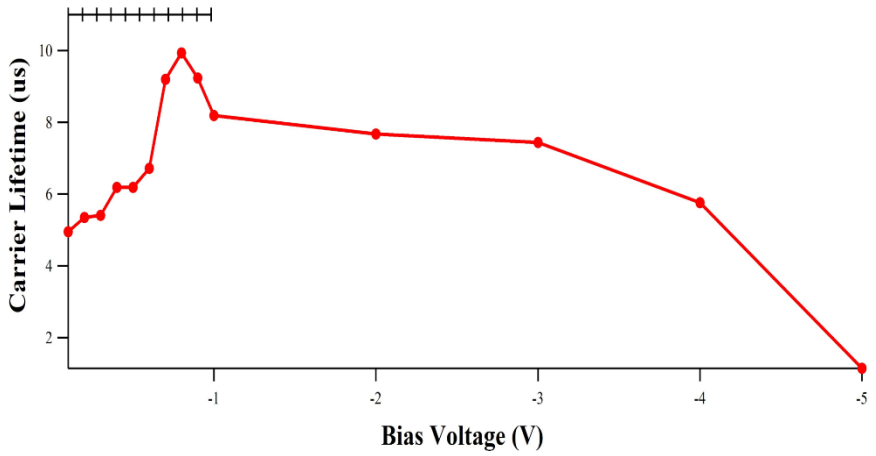

Figure 11 | Bias voltage dependence of the longest component in measured carrier lifetime signal. As it can be clearly seen, a non-linear behavior has been revealed, regarding to bias applied between 2 AFM cantilevers in contact mode.

Up to this stage, a conclusion can be drawn that the nanosecond OPP-STM system has been successfully developed, for probing carrier dynamics with 8ns temporal resolution. Furthermore, if high power laser (~100mW average output power would be enough) is used, then it would not be a far-fetched idea to implement this nanosecond OPP-STM to probe electron and nuclear spin dynamics in a user-and-budget-friendly way.